

Frequency Chirping of Energetic-Particle-Driven Geodesic Acoustic Modes in Tokamaks

R. Wu¹, A. Biancalani¹, D. Gossard², R. Ivanov^{3,1}, A. Mishchenko⁴,
X. Wang⁵, F. Zonca^{6,7}

¹ De Vinci Higher Education, De Vinci Research Center, Paris, France

² De Vinci Higher Education, Paris, France

³ Laboratoire de Physique des Plasmas, CNRS, Université Paris Saclay, Ecole Polytechnique,
Sorbonne Université, Observatoire de Paris, F-91120

⁴ Max Planck Institute for Plasma Physics, Greifswald, Germany

⁵ Max Planck Institute for Plasma Physics, 85748 Garching, Germany

⁶ Center for Nonlinear Plasma Science and C.R. ENEA Frascati, Via E. Fermi 45,
00044 Frascati, Italy

⁷ Institute for Fusion Theory and Simulation and Department of Physics,
Zhejiang University, Hangzhou 310027, China

March 25, 2026

Abstract

A suprathermal population of ions is present in tokamak plasmas due to external heating mechanisms and fusion reactions. These energetic particles (EP) can drive wave unstable, via inverse Landau damping. An example is the energetic-particle-driven geodesic acoustic mode (EGAMs). In this work, we perform a systematic gyrokinetic investigation of the EGAM linear and nonlinear dynamics, using the global gyrokinetic particle-in-cell code ORB5.

The nonlinear saturation given by the EP redistribution in phase space is characterized by a saturation level scaling quadratically with respect to the linear growth rate. The nonlinear EP dynamics in phase space has also effects on the EGAM frequency. To this extent, we investigate the frequency chirping, and we find that the chirping rate scales linearly with the linear growth rate over a wide range of EP concentrations. This scaling is consistent with the theoretical prediction of Chen-Zonca [L. Chen, and F. Zonca, Rev. Mod. Phys. 88, 015008 (2016)]

1 Introduction

Zonal (i.e. axisymmetric) flows (ZF), are mesoscale organized structures often observed in tokamaks in the presence of turbulence [1]. The characteristic polarization has the flow going along the poloidal direction, and a dependence on the minor radius of the tokamak, i.e. the direction of non-uniformity of the equilibrium temperature and density (no dependence on the toroidal angle due to the axisymmetry). Two kinds of ZF exist: zero-frequency ZF (ZFZF), and an oscillatory branch known as geodesic acoustic modes (GAMs) [2]. ZFZF are mainly damped by collisions, whereas GAMs are damped by both collisions and collisionless Landau damping [3, 4]. ZFs are key ingredients in the self-organization of turbulence in toroidal plasmas. Hence, the importance of understanding their dynamics, in order to have a comprehensive model of turbulent transport.

The presence of a population of energetic (i.e. suprathermal) particles (EPs), such as those generated by neutral beam injection or fusion-born α particles, qualitatively modifies this picture. Through inverse Landau damping, EP populations can destabilize GAMs, giving rise to EP-driven GAMs (EGAMs) [5]. EGAMs are of particular interest mainly because of their interaction with the EPs in phase space. They could also be mediators between turbulence, zonal flows, and energetic particles, and therefore influence transport and confinement [6].

Several contributions have been given to the construction of a theoretical model of EGAMs [5, 7, 8, 6, 9, 10, 11, 12]. Due to their nature of forced-oscillations, the dynamics of EGAMs strongly depends on the time evolution of the EP population in phase space. Not only their drive decreases when the velocity-gradient is depleted due to the nonlinear EP redistribution: also the frequency can change in time, during the nonlinear phase. This phenomenon, named frequency chirping, is a signature of the intrinsic nonlinear physics characterizing the EGAM interaction with EPs.

Frequency chirping is a known feature of many instabilities in nature. In tokamaks, it has been studied in detail for example for Alfvén modes [13, 14, 15, 16], and for fishbones [17]. In space, chorus waves have been also found to present a similar dynamics [18]. For EGAMs, frequency chirping has been observed in numerical simulations (see for example Ref. [19, 20, 21]) and compared with experiments (for example in Ref. [12]). Although GAMs and EGAMs are oscillations which exist only due to the magnetic field curvature [2], and therefore only in 2D shaped magnetic equilibrium, nevertheless, the EGAMs drive has a strong analogy with the beam plasma instability (BPI), which is a 1D physics phenomenon [7]. The beam plasma instability occurs when a plasma wave (also known as Langmuir wave) taps the free energy of a beam of energetic electrons, and becomes unstable due to inverse Landau damping. As a consequence, not only the linear excitation, but also the nonlinear saturation level of the EGAMs scales similarly to the BPI [20, 21]. The question remained unanswered so far is: what is the chirping rate scaling of EGAMs with respect to the linear growth rate? This question is important as the chirping rate scaling is intrinsically linked to the nature of the nonlinear saturation of the mode.

The present work addresses this issue, of how the EGAM frequency chirping rate depends on the linear properties of the mode. We investigate this problem by means of numerical simulations with the particle in cell code ORB5 [22]. ORB5 is a global

gyrokinetic code, written originally for turbulence studies. Gyrokinetics is the framework which is valid in the regime of frequencies which are much smaller than the ion cyclotron frequencies. In this regime, the fast gyro-motion of the particles can be averaged out, thus reducing the original 6D model to a 5D model. This allows faster numerical simulations. ORB5 is a multi-species code, and therefore it can be used to study EP-driven instabilities. We choose an EP distribution function of the shape of a bump-on-tail, i.e. a maxwellian shifted in the direction of the parallel velocity. For simplicity, the electrons are treated adiabatically here, as we wish to focus on the EP dynamics.

After validating the numerical framework with standard benchmarks, we investigate how the linear growth rate, nonlinear saturation level, and frequency chirping of EGAMs depend on the energetic particle concentration. The quadratic scaling of the saturation level with the linear growth rate is recovered, as given in Ref. [20]. Regarding the frequency chirping rate, we obtain a linear scaling with respect to the linear growth rate. Note that this is different with respect to the BPI, where the frequency displacement with respect to the linear frequency is expected to evolve like $\delta\omega \propto \sqrt{t}$ [23]. We explain this difference between EGAMs and the BPI, by recalling that, in the regime considered here, EGAMs exhibit a non-adiabatic saturation [20] (whereas the BPI is usually explained in the adiabatic regime). On the other hand, note that this scaling of the chirping rate going linearly with the linear growth rate, can be explained with the theoretical prediction given by Chen & Zonca [15], similarly to what found for Alfvén modes [16, 24].

The paper is organized as follows. Section 3 recalls the theoretical background on GAMs, Landau damping, and EGAMs. The model equilibrium and numerical setup are described in Section 4. Simulation results are presented in Section 5, followed by a summary and discussion in Section 6.

2 Theoretical Background

2.1 Geodesic Acoustic Modes

GAMs are axisymmetric oscillations of the zonal $\mathbf{E} \times \mathbf{B}$ flow, whose restoring force originates from the geodesic curvature of the magnetic field [2]. When a flux-surface-averaged radial electric field perturbation is generated, the associated $\mathbf{E} \times \mathbf{B}$ flow induces a compression of the plasma density on the flux surface. The resulting density perturbation drives parallel currents, which react back on the radial electric field, forming a closed feedback loop that sustains oscillatory dynamics.

In thermal plasmas, GAMs oscillate at an acoustic frequency of order

$$\omega_{\text{GAM}} = \frac{\sqrt{2} c_s}{R_0}, \quad (1)$$

where c_s is the ion sound speed and R_0 is the major radius of the tokamak. Kinetic effects, in particular ion Landau damping, lead to strong attenuation of GAMs in Maxwellian plasmas.

2.2 Energetic-Particle-Driven GAMs

When energetic particles (EPs) are present, the dynamics change qualitatively. Non-Maxwellian EP velocity distributions, such as the double bump-on-tail profiles shown in Figure 2, can provide a positive velocity-space gradient near resonance, enabling energy transfer from particles to the wave through inverse Landau damping. Consequently, GAMs can become unstable, giving rise to EGAMs [20]. In nonlinear simulations, the growth is eventually arrested and the mode saturates at a finite amplitude; the saturation physics is discussed in Sec. 5.

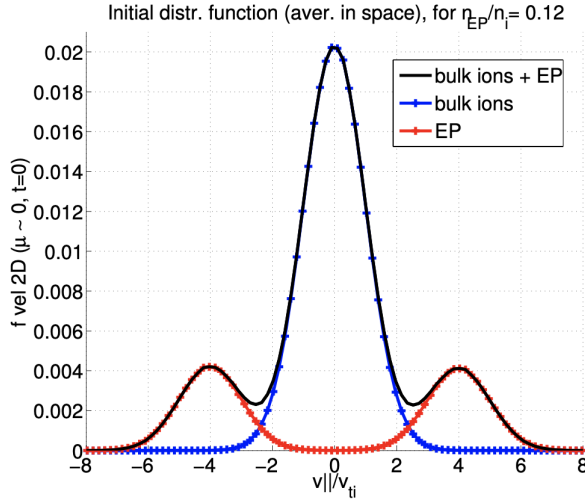


Figure 1: Initial EP symmetric bump-on-tail distribution function for a simulation with $n_{EP}/n_i = 0.12$, $v_{bump}/v_{ti} = 4$. Reproduced from Biancalani et al. (2017) [20]

3 Model and Equilibrium

3.1 Tokamak Equilibrium and Plasma Profiles

In this work, we adopt the simplified tokamak equilibrium configuration used in Refs. [20, 21]. The system consists of a circular cross-section tokamak without Shafranov shift, designed to isolate the essential physics of GAMs and EGAMs.

The major radius is set to $R_0 = 1$ m and the minor radius to $a = 0.3125$ m. The magnetic field on axis is $B_0 = 1.9$ T. A flat safety factor profile with $q = 2$ is considered, corresponding to circular flux surfaces without equilibrium current effects.

Both density and temperature profiles of the thermal plasma are assumed to be flat. The plasma temperature is specified through the normalized ion sound Larmor radius

$$\rho^* = \frac{\rho_s}{a} = \frac{1}{128} \simeq 0.0078, \quad (2)$$

where

$$\rho_s = \frac{c_s}{\Omega_i}, \quad c_s = \sqrt{\frac{T_e}{m_i}}, \quad (3)$$

with ρ_s is the ion sound Larmor radius, Ω_i the ion cyclotron frequency, m_i the ion mass, and T_e the electron temperature.

Assuming equal ion and electron temperatures, $T_e = T_i$ ($\tau = T_e/T_i = 1$), and a hydrogen plasma, the corresponding physical values are

$$T_i \simeq 2060 \text{ eV}, \quad \Omega_i = 1.82 \times 10^8 \text{ rad/s}, \quad c_s = 4.44 \times 10^5 \text{ m/s}. \quad (4)$$

The associated sound frequency is

$$\omega_s = \frac{\sqrt{2} c_s}{R_0} = 6.28 \times 10^5 \text{ rad/s}. \quad (5)$$

Energetic particles (EPs) are initialized using a symmetric bump-on-tail distribution function, characterized by two peaks in the parallel velocity at

$$v_{\parallel} = \pm v_{\text{bump}}, \quad v_{\text{bump}} = 4v_{ti}, \quad (6)$$

where

$$v_{ti} = \sqrt{\frac{T_i}{m_i}} \quad (7)$$

is the ion thermal velocity. The EP distribution depends only on constants of motion, and radial variations of the magnetic field are neglected in the initialization.

Neumann and Dirichlet boundary conditions are imposed on the electrostatic potential at the inner and outer boundaries, corresponding to $s = 0$ and $s = 1$, respectively. As the EP concentration is increased, the system transitions smoothly from a damped GAM to an unstable EGAM.

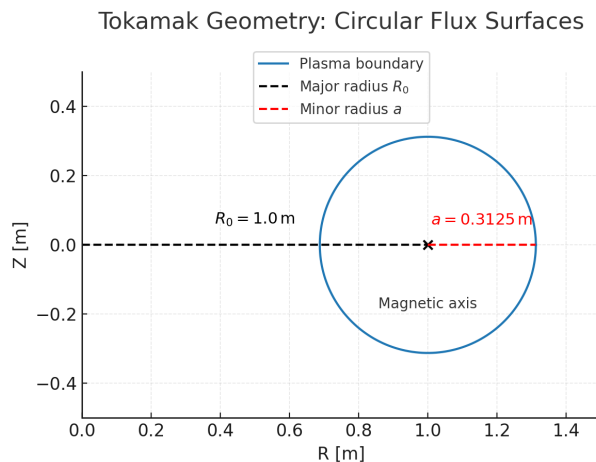


Figure 2: Tokamak geometry with $R_0 = 1 \text{ m}$, $a = 0.3125 \text{ m}$

3.2 The ORB5 Gyrokinetic Code

Simulations are performed using the global gyrokinetic particle-in-cell (PIC) code ORB5 [22]. An electrostatic model with adiabatic electrons is employed, following Refs.[20].

In this framework, particle trajectories are evolved self-consistently in five-dimensional phase space together with the electrostatic fields, allowing the description of the linear growth, nonlinear saturation, and frequency chirping of energetic-particle-driven GAMs.

3.3 Signal Processing and Diagnostic Methods

To analyze the temporal evolution of EGAMs, the flux-surface-averaged electrostatic potential $\bar{\phi}(t)$ is first extracted from the simulations. The corresponding radial electric field is then computed as

$$E_r(t) = -\partial_r \bar{\phi}(t), \quad (8)$$

which serves as the primary diagnostic quantity throughout this work.

The linear growth rate γ_L is determined by fitting the exponential growth phase of the signal on a semi-logarithmic scale. A linear regression of the early-time interval provides a direct estimate of γ_L .

To investigate the nonlinear frequency dynamics, the time–frequency evolution of $E_r(t)$ was analyzed using the continuous wavelet transform (CWT). The CWT method provides a localized spectral decomposition, allowing the clear identification of mode frequencies as they evolve in time, and is particularly suitable for capturing the chirping behavior characteristic of EGAMs. The instantaneous frequency was obtained by following the ridge of maximum wavelet amplitude, and the chirping rate was estimated by applying a linear regression to the extracted frequency trajectory.

4 Simulation Results

4.1 GAM Benchmark

4.1.1 Rosenbluth–Hinton Test

As a preliminary validation, simulations without energetic particles were performed. Following the initialization of a zonal radial electric field, damped GAM oscillations around a finite residual level are observed, in agreement with the Rosenbluth–Hinton theory. This confirms that ORB5 correctly captures the linear GAM and zonal-flow dynamics in the present configuration.

4.1.2 GAM Frequency and Damping

After validating the numerical framework, we characterize the GAM oscillation properties in the simplified tokamak configuration described in Sec. 4.1. A zonal radial electric field perturbation is initialized and its temporal evolution is monitored.

The GAM frequency is extracted from the dominant oscillatory component of the signal during the early-time oscillations. Using peak detection, we obtain $\omega_{\text{sim}} \simeq 1.7\omega_s$, where $\omega_s = \sqrt{2}c_s/R_0$ is the sound frequency. This value is consistent, at the order-of-magnitude level, with kinetic GAM frequency estimates reported in Sugama and Watanabe (2006) [25].

The damping rate is evaluated from the exponential decay of the oscillation envelope. By fitting the logarithm of the oscillation amplitude, a damping rate $\gamma \simeq 1.1 \times 10^{-4} \omega_i$ is obtained, confirming that GAMs are strongly damped in the absence of energetic particles.

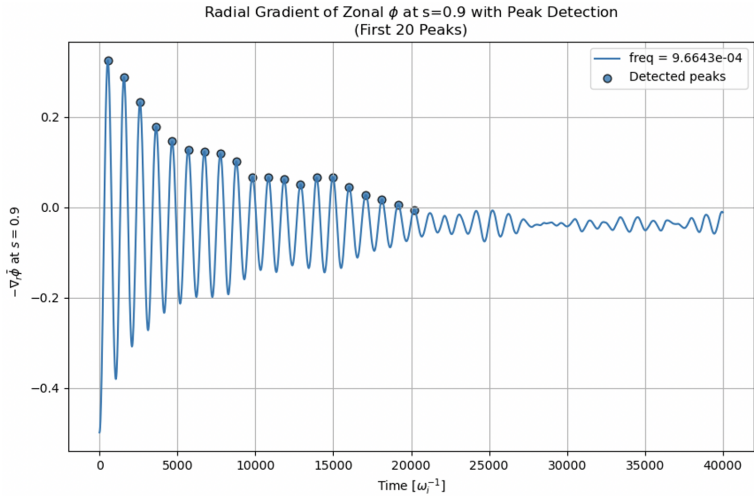


Figure 3: Temporal evolution of the radial electric field perturbation at $s = 0.9$, showing damped GAM oscillations.

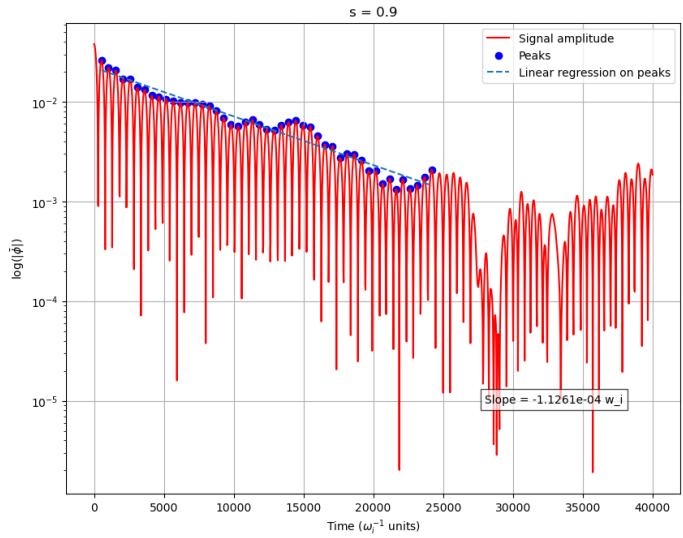


Figure 4: Logarithmic fit of the GAM oscillation envelope at $s = 0.9$, used to evaluate the damping rate.

4.2 EGAM

4.2.1 Radial Electric Field and Frequency Evolution: Linear vs Nonlinear Regimes

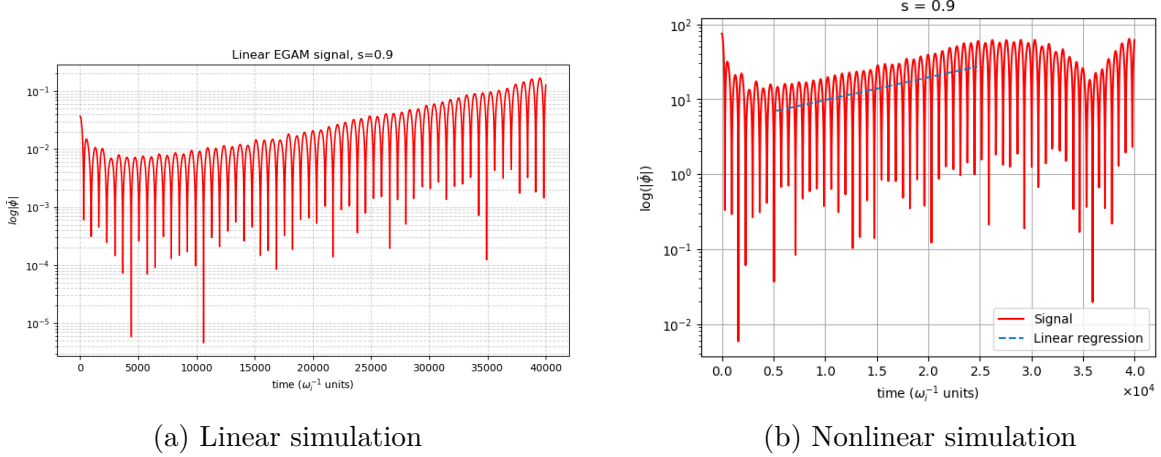


Figure 5: Time evolution of the radial electric field $E_r(t)$ at $s = 0.9$ with an EP concentration of 7%. Panel (a) corresponds to the linear simulation, while panel (b) corresponds to the nonlinear simulation.

To illustrate the fundamental features of EGAMs under different simulation conditions, we first show the time evolution of the radial electric field in both linear and nonlinear simulations.

In the linear simulation (see Figure 5a), the amplitude of the radial electric field exhibits an almost perfect exponential growth. This behavior is fully consistent with linear theory, where the mode freely grows under the EP drive without being affected by nonlinear effects. Such signals are particularly suitable for the measurement of the linear growth rate γ_L , since the exponential growth region can be accurately captured by logarithmic linear fitting. It should be noted that, during this stage, the mode frequency remains constant and no chirping phenomenon is observed.

In contrast, in the nonlinear simulation (see Figure 5b), the time evolution of the radial electric field exhibits significantly different characteristics. The mode also undergoes an initial exponential growth, but once the amplitude reaches a certain level, the exponential law breaks down and the system enters the nonlinear stage. In this regime, the mode amplitude saturates at a finite level, often accompanied by frequency chirping in the electric field signal. These features are direct evidence of nonlinear wave-particle interactions.

It should be noted that the initial amplitudes of the signals in the linear and nonlinear simulations are not identical. This difference does not reflect a change in the physical setup, but rather originates from an internal adjustment performed by ORB5 on the imposed initial perturbation. Specifically, if the perturbation were too large, the system would immediately enter the nonlinear stage, skipping the linear exponential growth phase. To avoid this unphysical behavior and to ensure that the mode first evolves in the linear

regime, ORB5 automatically rescales the initial perturbation. As a result, a small offset in the early-time amplitude appears between the linear and nonlinear cases, while the subsequent growth dynamics remain unaffected.

This conclusion is further supported by the time–frequency analysis. Figure 6 presents the frequency evolution of the $E_r(t)$ signal extracted via continuous wavelet transform (CWT). In the beginning stage of the EGAM signal, the mode frequency remains nearly constant, corresponding to the linear growth phase of the radial electric field. However, when the time approaches $t \simeq 29000 \Omega_i^{-1}$, the frequency starts to evolve in time, indicating the onset of chirping. Remarkably, this moment coincides with the radial electric field entering saturation in nonlinear simulations, showing that chirping starts as the system becomes nonlinear.

Based on these observations, in the following sections we quantitatively investigate the relations among the linear growth rate, the nonlinear saturation level, and the chirping rate, aiming to uncover the fundamental scaling laws that characterize the nonlinear dynamics of EGAMs.

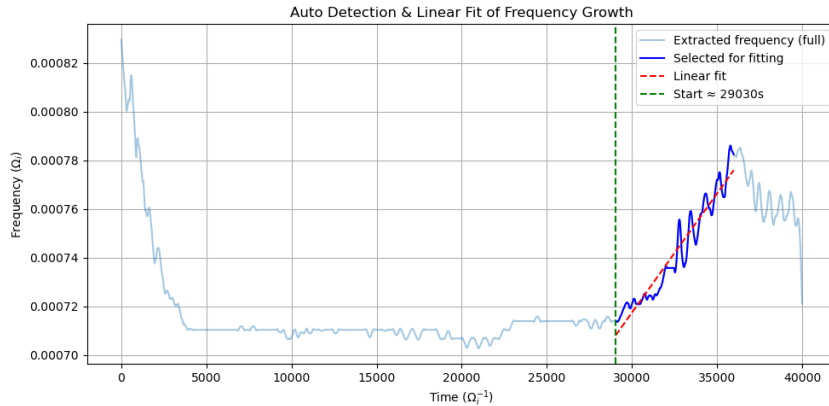
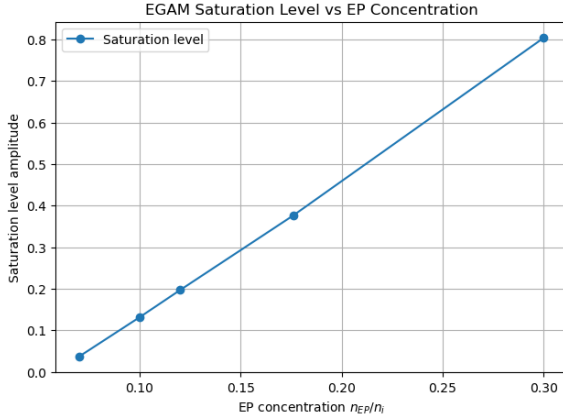


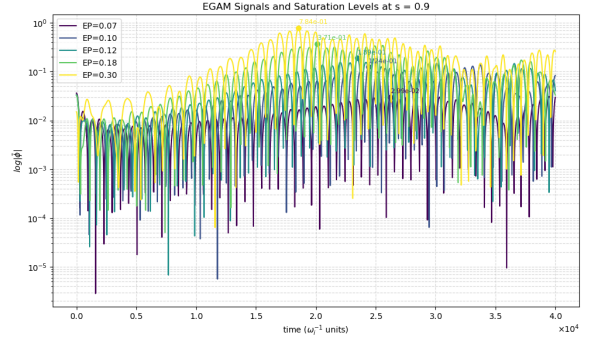
Figure 6: Time–frequency representation of the $E_r(t)$ signal at $s = 0.9$ with an EP concentration of 7%, obtained via continuous wavelet transform (CWT). One can notice that in the very beginning of the signal ($t = 0$ to $t \simeq 5000 \Omega_i^{-1}$), the frequency appears to decrease. This feature is not of physical origin, but rather an artifact introduced by the CWT signal processing, and can therefore be safely neglected. Around $t \simeq 29000 \Omega_i^{-1}$, the frequency starts to drift, indicating the onset of chirping.

4.2.2 Dependence of Linear Growth Rate and Saturation Level on EP Concentration

We now examine the dependence of the EGAM saturation amplitude on the EP concentration. As shown in Figure 7, the saturation level systematically increases with EP concentration. The onset of saturation can be attributed to nonlinear wave–particle interactions: once the mode amplitude grows sufficiently, resonant EPs are redistributed in velocity space, thereby reducing the available free energy and limiting further growth. With higher EP concentration, however, the stronger drive allows the system to sustain a larger nonlinear equilibrium amplitude.



(a) Saturation amplitude as a function of EP concentration.



(b) Time evolution of EGAM signals at different EP concentrations, with the corresponding saturation levels.

Figure 7: Dependence of EGAM saturation level on EP concentration. Panel (a) shows the saturation amplitude as a function of EP concentration n_{EP}/n_i , demonstrating that stronger EP drive sustains a higher nonlinear equilibrium amplitude. Panel (b) presents the time evolution of EGAM signals at different EP concentrations ($s = 0.9$), where the saturation levels are extracted from the maximum amplitude of the oscillations.

This nonlinear saturation mechanism is consistent with the gyrokinetic theory of Qiu et al. (2011)[26], indicating that a stronger energetic particle drive is able to sustain a higher nonlinear equilibrium amplitude. This behaviour is consistent with previous theoretical and numerical studies of A.Biancalani et al.[20], which demonstrated that the saturated electric field of EGAMs scales quadratically with the linear growth rate, i.e.

$$\delta E_r \propto \gamma_L^2 \quad (9)$$

Even in the high-drive regime, where nonlinear frequency chirping may occur, this quadratic scaling law remains valid [21].

Furthermore, Figure 8 shows that γ_L increases with the EP concentration. In the low-concentration regime, although the absolute values of the growth rate remain small, the slope of the curve is relatively steep, indicating that the growth rate is highly sensitive to variations in EP concentration. In the high-concentration regime, the growth rate reaches larger values, but its incremental increase becomes weaker. Overall, the data points form an increasing curve, clearly revealing the general trend that the growth rate is enhanced as the EP concentration increases.

This trend can be understood as the competition between thermal-ion Landau damping and EP inverse Landau damping: higher EP concentration strengthens the positive velocity-space gradient near the resonance, thereby providing stronger drive and counteracting the damping from thermal ions. This physical mechanism has been discussed and verified in the studies by Zonca and Chen (2015)[27], Qiu et al.[26] (2011), and Biancalani et al. (2017)[20].

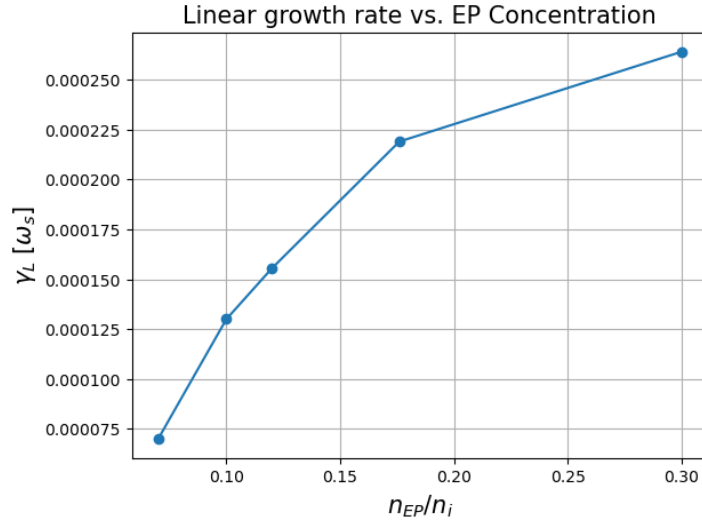


Figure 8: Linear growth rate vs EP concentration at $s = 0.9$.

In summary, the EP concentration not only controls the linear growth rate of EGAMs, but also determines the nonlinear saturation amplitude. The two quantities are closely linked through a quadratic scaling law, $\delta E_r \propto \gamma_L^2$, which remains valid even in regimes where frequency chirping occurs. These results highlight the fundamental role of EP drive in governing both the linear and nonlinear dynamics of EGAMs, and provide the basis for the following analysis of chirping phenomena.

4.2.3 Dependence of Chirping Rate and Saturation Level on EP Concentration

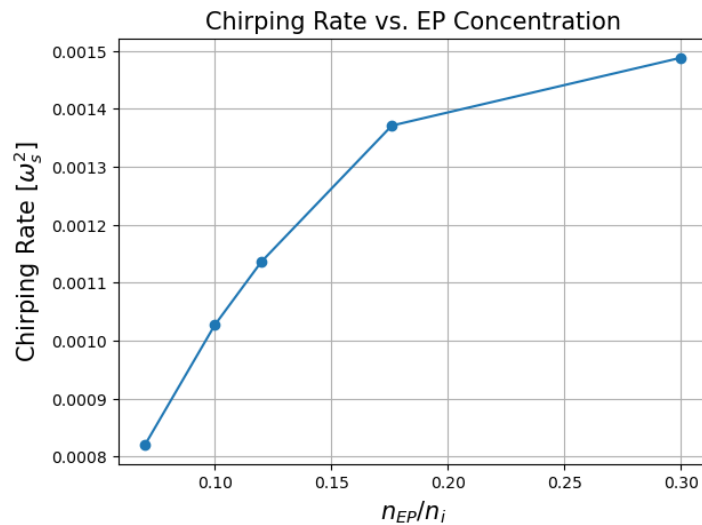


Figure 9: Chirping rate versus EP concentration at $s = 0.9$.

Figure 9 shows the dependence of the chirping rate on the EP concentration. A clear

systematic trend is observed: as the EP drive becomes stronger, the frequency sweeping accelerates. At low EP concentrations, the chirping rate remains relatively small in magnitude, but already exhibits a pronounced sensitivity to variations in the fast-particle population. As the EP concentration is further increased, the chirping rate attains significantly larger values, consistent with the stronger drive. However, the incremental enhancement gradually diminishes, reflecting the increasing role of nonlinear phase-space redistribution. This behavior mirrors the qualitative trend of the linear growth rate, yet it carries a distinct physical meaning: while γ_L characterizes the strength of the linear instability, the chirping rate directly quantifies the pace of nonlinear wave-particle interactions and the resulting frequency evolution.

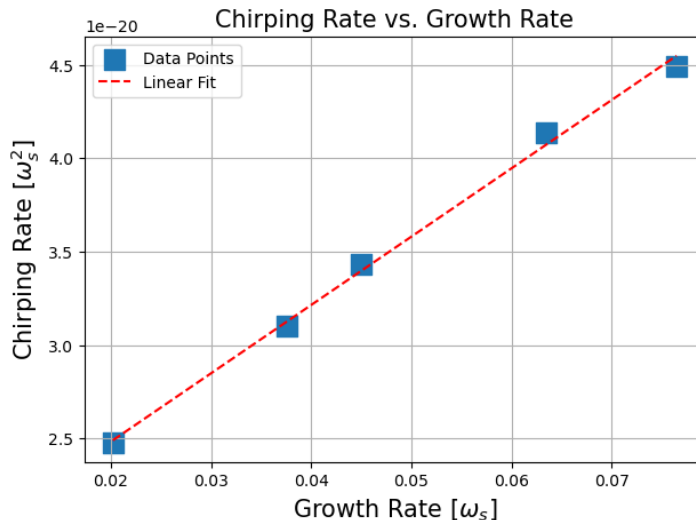


Figure 10: Chirping rate versus growth rate.

The simulation results consistently show that the linear growth rate γ_L increases with the EP concentration. At the same time, the chirping rate exhibits the same increasing trend, indicating a direct connection between the two quantities. Most importantly, as illustrated in Figure 10, the chirping rate is found to scale linearly with the linear growth rate.

These numerical findings are in close agreement with the existing theoretical framework. Chen and Zonca (2016, RMP)[15] demonstrated that the scaling of the chirping rate is determined by the wave-particle trapping dynamics, predicting a proportionality between the chirping rate and the linear growth rate γ_L . Their unified fishbone paradigm encompasses both adiabatic and nonadiabatic chirping, and emphasizes the crucial role of nonperturbative energetic particle responses in governing the nonlinear frequency evolution.

Building on this theoretical foundation, Xin Wang et al. (2023)[16] performed systematic nonlinear simulations of Alfvén modes (TAE/EPM) using the global gyrokinetic code ORB5, and verified this prediction for the first time. Their results showed that, independent of whether the EP drive was modified by varying the EP density or the background temperature gradient, the chirping rate consistently exhibited a linear scaling with the

saturation amplitude of the mode.

Within this context, our EGAM simulations provide a new and important extension. We demonstrate that, even for an acoustic branch mode, the chirping rate exhibits a clear linear scaling with the linear growth rate γ_L . This constitutes the first systematic evidence that the universal scaling law, previously established for Alfvénic modes, also applies to EGAMs. By extending the applicability of the Chen–Zonca theoretical framework, our findings highlight the universal nature of nonadiabatic wave–particle interactions across different branches of plasma modes. This result fills a critical gap in the understanding of nonlinear EGAM dynamics, where energetic particle effects are expected to play a dominant role.

5 Summary and Discussion

In this work, we have performed a systematic gyrokinetic investigation of energetic-particle-driven geodesic acoustic modes (EGAMs) in a simplified tokamak equilibrium using the global gyrokinetic code ORB5.

The simulations show that, as the energetic particle (EP) drive increases, EGAMs undergo a transition from linear exponential growth to a nonlinear regime characterized by finite-amplitude saturation and frequency chirping. The nonlinear saturation level is found to scale quadratically with the linear growth rate, consistent with previous theoretical and numerical studies based on nonlinear phase-space redistribution of resonant particles.

Most importantly, the frequency chirping rate is shown to scale linearly with the linear growth rate over a wide range of EP concentrations. This provides the first systematic numerical evidence that the universal chirping scaling law predicted by the Chen–Zonca theoretical framework—previously validated for Alfvénic modes—also applies to acoustic-branch modes such as EGAMs. These results extend the applicability of nonperturbative wave–particle interaction theory beyond the Alfvénic spectrum and support its universal character.

Future work will consider more realistic configurations, including shaped equilibria, electromagnetic effects, and experimentally relevant energetic particle distributions, in order to establish closer connections between the present results and observations in current and next-generation tokamaks.

6 Acknowledgments

The authors gratefully acknowledge stimulating and fruitful discussions with Philipp Lauber, Alberto Bottino, Thomas Hayward-Schneider, Ningfei Chen, and the entire ORB5 team, which provided valuable perspectives and significantly enriched this work. This work has been carried out within the framework of the EUROfusion Consortium, partially funded by the European Union via the Euratom Research and Training Programme (Grant Agreement N° 101052200 — EUROfusion). This research was supported by computational resources provided by the Leonardo supercomputer at CINECA.

References

- [1] A. Hasegawa, C. G. MacLennan, and Y. Kodama. “Nonlinear behavior and turbulence spectra of drift waves and Rossby waves”. In: *Physics of Fluids* 22 (Nov. 1979), pp. 2122–2129. DOI: 10.1063/1.862504.
- [2] Niels Winsor, John L. Johnson, and John M. Dawson. “Geodesic Acoustic Waves in Hydromagnetic Systems”. In: *Physics of Fluids* 11.11 (1968), pp. 2448–2450. DOI: 10.1063/1.1691835.
- [3] L. D. Landau. “On the vibration of the electronic plasma”. In: *Journal of Physics (USSR)* 10 (1946). English translation of Zh. Eksp. Teor. Fiz. 16 (1946), 574; reprinted in *Collected Papers of L. D. Landau*, ed. D. ter Haar, Pergamon Press, 1965, pp. 445–460, pp. 25–34.
- [4] W. Herr. “Introduction to Landau Damping”. In: *Proceedings of the CAS-CERN Accelerator School: Advanced Accelerator Physics, Trondheim, Norway, 19–29 August 2013*. Ed. by W. Herr. Vol. CERN-2014-009. CERN Yellow Reports. Geneva: CERN, 2014. DOI: 10.5170/CERN-2014-009.137.
- [5] G. Y. Fu. “Energetic-Particle-Induced Geodesic Acoustic Mode”. In: *Physical Review Letters* 101.18, 185002 (Oct. 2008), p. 185002. DOI: 10.1103/PhysRevLett.101.185002.
- [6] D. Zarzoso et al. “Impact of Energetic-Particle-Driven Geodesic Acoustic Modes on Turbulence”. In: *Physical Review Letters* 110.12, 125002 (Mar. 2013), p. 125002. DOI: 10.1103/PhysRevLett.110.125002.
- [7] Z. Qiu, F. Zonca, and L. Chen. “Nonlocal theory of energetic-particle-induced geodesic acoustic mode”. In: *Plasma Physics and Controlled Fusion* 52.9, 095003 (Sept. 2010), p. 095003. DOI: 10.1088/0741-3335/52/9/095003.
- [8] Z. Qiu, F. Zonca, and L. Chen. “Kinetic theories of geodesic acoustic modes: Radial structure, linear excitation by energetic particles and nonlinear saturation”. In: *Plasma Science and Technology* 13.3 (2011), p. 257.
- [9] K. Miki and Y. Idomura. “Finite-Orbit-Width Effects on Energetic-Particle-Induced Geodesic Acoustic Mode”. In: *Plasma and Fusion Research* 10 (2015), pp. 3403068–3403068. DOI: 10.1585/pfr.10.3403068.
- [10] M. Sasaki et al. “A branch of energetic-particle driven geodesic acoustic modes due to magnetic drift resonance”. In: *Physics of Plasmas* 23.10, 102501 (Oct. 2016), p. 102501. DOI: 10.1063/1.4963397.
- [11] M. Sasaki et al. “Toroidal momentum channeling of geodesic acoustic modes driven by fast ions”. In: *Nuclear Fusion* 57.3, 036025 (Mar. 2017), p. 036025. DOI: 10.1088/1741-4326/aa4eb4.
- [12] I. Novikau et al. “Nonlinear dynamics of energetic-particle driven geodesic acoustic modes in ASDEX Upgrade”. In: *Physics of Plasmas* 27.4, 042512 (Apr. 2020), p. 042512. DOI: 10.1063/1.5142802. arXiv: 1912.07950 [physics.plasm-ph].

- [13] A. Fasoli et al. “Nonlinear Splitting of Fast Particle Driven Waves in a Plasma: Observation and Theory”. In: *Phys. Rev. Lett.* 81 (25 Dec. 1998), pp. 5564–5567. DOI: 10.1103/PhysRevLett.81.5564. URL: <https://link.aps.org/doi/10.1103/PhysRevLett.81.5564>.
- [14] S D Pinches et al. “The role of energetic particles in fusion plasmas”. In: *Plasma Physics and Controlled Fusion* 46.12B (Nov. 2004), B187. DOI: 10.1088/0741-3335/46/12B/017. URL: <https://doi.org/10.1088/0741-3335/46/12B/017>.
- [15] Liu Chen and Fulvio Zonca. “Physics of Alfvén waves and energetic particles in burning plasmas”. In: *Reviews of Modern Physics* 88.1 (2016). Published 23 March 2016, p. 015008. DOI: 10.1103/RevModPhys.88.015008.
- [16] X. Wang et al. “Nonlinear dynamics of nonadiabatic chirping-frequency Alfvén modes in tokamak plasmas”. In: *Plasma Physics and Controlled Fusion* 65.7 (2023), p. 074001. DOI: 10.1088/1361-6587/acd71f.
- [17] G. Brochard et al. “Saturation of fishbone instability through zonal flows driven by energetic particle transport in tokamak plasmas”. In: *Nuclear Fusion* 65.1 (Dec. 2024), p. 016052. DOI: 10.1088/1741-4326/ad8013. URL: <https://doi.org/10.1088/1741-4326/ad8013>.
- [18] Xin Tao et al. “Theoretical and numerical studies of chorus waves: A review”. In: *Science China Earth Sciences* 63.1 (Jan. 2020), pp. 78–92. DOI: 10.1007/s11430-019-9384-6.
- [19] H. Wang, Y. Todo, and C. C. Kim. “Hole-Clump Pair Creation in the Evolution of Energetic-Particle-Driven Geodesic Acoustic Modes”. In: *Physical Review Letters* 110.15, 155006 (Apr. 2013), p. 155006. DOI: 10.1103/PhysRevLett.110.155006.
- [20] A. Biancalani et al. “Saturation of energetic-particle-driven geodesic acoustic modes due to wave–particle nonlinearity”. In: *Journal of Plasma Physics* 83.6 (2017), p. 725830602. DOI: 10.1017/S0022377817000976.
- [21] A. Biancalani et al. “Nonlinear velocity redistribution caused by energetic-particle-driven geodesic acoustic modes, mapped with the beam-plasma system”. In: *Journal of Plasma Physics* 84 (2018), p. 725840602. DOI: 10.1017/S002237781800123X.
- [22] E. Lanti et al. “ORB5: A global electromagnetic gyrokinetic code using the PIC approach in toroidal geometry”. In: *Computer Physics Communications* (2019). DOI: 10.1016/j.cpc.2019.107072.
- [23] M. Lesur, Y. Idomura, and X. Garbet. “Fully nonlinear features of the energetic beam-driven instability”. In: *Physics of Plasmas* 16.9, 092305 (Sept. 2009), p. 092305. DOI: 10.1063/1.3234249.
- [24] Andreas Bierwage, Roscoe B. White, and Vinícius N. Duarte. “On the Effect of Beating during Nonlinear Frequency Chirping”. In: *Plasma and Fusion Research* 16 (July 2021), pp. 1403087–1403087. DOI: 10.1585/pfr.16.1403087. arXiv: 2103.12561 [physics.plasm-ph].

- [25] H. Sugama and T.-H. Watanabe. “Collisionless damping of geodesic acoustic modes”. In: *Journal of Plasma Physics* 72.6 (2006). Received 10 August 2005; accepted 7 January 2006, pp. 825–828. DOI: 10.1017/S0022377806004958.
- [26] Zhiyong Qiu, Fulvio Zonca, and Liu Chen. “Kinetic Theories of Geodesic Acoustic Modes: Radial Structure, Linear Excitation by Energetic Particles and Nonlinear Saturation”. In: *Plasma Science and Technology* 13.3 (2011), pp. 257–267. DOI: 10.1088/1009-0630/13/3/01.
- [27] F. Zonca et al. “Nonlinear dynamics of phase space zonal structures and energetic particle physics in fusion plasmas”. In: *New Journal of Physics* 17 (2015), p. 013052. DOI: 10.1088/1367-2630/17/1/013052.